Burn-out, circumferential film flow distribution and pressure drop for an eccentric annulus with heated rod

Andersen, P.S.; Jensen, A.; Mannov, G.; Olsen, A.

Publication date:
1973

Document Version
Publisher's PDF, also known as Version of record

A. E. K. Risø

Risø - M - 1623

Risø - M - 1623

Title and author(s)

BURN-OUT, CIRCUMFERENTIAL FILM FLOW DISTRIBUTION AND PRESSURE DROP FOR AN ECCENTRIC ANNULUS WITH HEATED ROD

by

P. S. Andersen

A. Jensen

C. Mannov

A. Olsen

Date May 1973

Department or group Reactor Physic

Group's own registration number(s)

12 pages + 3 tables + 23 illustrations

Abstract

Measurements of

1. Burn-out,
2. Circumferential film flow distribution and
3. Pressure drop

in a 17*27.2*3500 mm annulus geometry are reported in this preliminary report. The eccentricity was varied between 0 and 3 mm. The pressure and rod heat flux were held constant at 70 bar and 100.7 W/cm^2. Burn-out curves are presented for mass velocities between 200 and 1500 kg/m^{2}s and for inlet subcoolings of 10 °C and 100 °C. The film flow and pressure drop measurements correspond to the steam qualities x ≙ 19 % and 24 % for the mass velocity G = 602 kg/m^{2}s and x ≙ 20 % and 23 % for G = 1200 kg/m^{2}s.

The influence of the circumferential rod film flow variation on burn-out is discussed.

Copies to

Library 100

Editors 80

Abstract to

Available on request from the Library of the Danish Atomic Energy Commission (Atomenergikommissionens Bibliotek), Risø, Roskilde, Denmark.
Telephone: (03) 35 51 01, ext 334, telex: 5072.

FI 25-204

ISBN 87 550 0201 3

CONTENTS.

1. Introduction.

The present investigation is a part of a joint project "The Scandinavian Subchannel Project" between AEC, Risø, AB Atomenergi, Sweden and IFA, Norway with the goal of developing reliable prediction methods based upon subchannel analysis for diabatic two-phase flows. One objective is to perform burn-out predictions in rod clusters by means of a "film-flow model" capable of taking into account variations in mass velocities and heat fluxes along the rods and also mutual interactions of the rods and the rods and the shroud.

The present diabatic steam-water experimental programme was primarily designed to answer some basic questions on the relationship between film flow rate and burn-out under asymmetrical conditions.

Experimental film flow measurements in eccentric annuli with air-water mixtures have been reported by Butterworth [1] and Schraub et al. [2]. Both experimenters found that the circumferential variation in the rod film flow rate was very small.

2. Experimental Equipment and Procedure.

The experiments were carried out in the o.8 MW loop of the Laboratory of Reactor Technology at KTH in Stockholm. For a detailed description of this loop see ref. [3].

The annular test section consists of a directly heated 17 mm stainless steel rod mounted inside a 27.2 mm i.d. unheated stainless steel tube. The heated length of the rod is 3500 mm. The rod can be mounted in positions corresponding to the eccentricities, E = o, o.75, 1.5, 2.5 and 3.o mm. The outer tube is provided with holes for spacers, axial pressure drop distribution measurements and needle contact probes (for the measurements of the axial film thicknesses; these measurements are not reported herein).

The rod film may be sucked off through suction holes beginning lo mm above the end of the heated length. The tube film is sucked off through suction holes at the same level. During three experimental periods (period 3, 4 and 5) the geometry of the perforated areas were as indicates in table 1.

Exp. period	Rod perforation		Tube perforation		No. of spacers per level
	Fraction of perimeter perforated	Comment	Fraction of perimeter perforated	Comment	
3	360 °	560, 1.2 mm holes over a length of 51 mm	360 °	920, 1.6 mm holes over a length of 55 mm	3
4	62.3°	See Fig. 1.	62.9°	See Fig. 2	4
5					

Table 1. Geometrical data for 17×27.2×3500 mm test section.

The steam-water mixtures extracted through rod and tube perforations were condensed in separate heat exchangers and metered by venturis or orifices. The relative amounts of steam and water were determined by heat balances. Rod and tube suctions were not performed simultanously.

The relative positions of the rod and tube perforations, which have been realized experimentally, are summerized in the sketch Fig. 3. Note that only in "position 2.5" for concentric annulus the two perforations are not "facing" each other.

The spacers were 2 mm dia. pins with semi-spherical tips mounted radially on the tube.

There were 500 mm between spacer levels. Tabel 1 indicates the number of pins per spacer level for the three experimental periods.

3. Results.

3.1. Burn-Out.

Fig. 4 summarizes all the burn-out measurements on concentric and eccentric annulus. The graph gives the total burn-outer power Q_{BO} as a function of the mass velocity G for the subcoolings Δt_{sub} = 10 °C and Δt_{sub} = 100 °C. For each subcooling the eccentricity, E is a parameter. It is clear that burn-out is adversly affected by eccentricity for G > 500 kg/m^{2}s. For smaller mass velocities the effect may be reversed (at least for the larger subcooling). The burn-out measurements were performed during experimental period no. 5.

3.2. Film Flow.

In general a two-phase mixture is being sucked out through the perforation in tube and rod. Plotting the sucked out water flow rate, $\dot{m}_w$, versus the steam flow rate, $\dot{m}_s$, one obtains a "suction curve". Examples are shown in Figs. 5 and 6 for rod and tube respectively. The shape of the suction curves reflects the steam content in the film, the waviness of the film surface and the water content in the core. For the present purpose the "film flow rate", $\dot{m}_f$, is defined by a straight line extrapolation to $\dot{m}_s$ = 0 (The dotted lines in Figs. 5 and 6 are examples of the method of extrapolation). Fig. 7 presents suction curves for rod obtained for concentric annulus (E=0) under various experimental conditions. We note that there is very good agreement between experiments with a 62.3° perforation. In particular : 1) Fin

geometry is of no significance (compare results for experimental periods 4 and 5), 2) Turning the perforation by 90° (pos. 2.5) does not alter the results. This is taken to indicate that the film is evenly distributed around the rod for concentric conditions.

However, comparing suction results from a fraction of the perimeter (i. e. 62.3 °) with results from suction from the total perimeter one notes a marked difference. The film flow rate deduced from "total suction" is unexplainally lower (by ≈ 20 %) than that from "partial suction". It might be speculated that water deposited on the fins accounts for the difference. However, the two sets of fins (one 0.5 mm in height the other 1.0 mm) gave identical results. Fig. 8 similarly displays tube suction curves for concentric annulus for three cases of "partial" suction (62.9°)and one case of suction from the total perimeter. Good agreement is found between all the results.

The experimental data for rod film flow are summarized in table 2. Figs. 9 through 12 display the angular (circumferential) distribution of rod film flow. The results are presented as the film flows corresponding to suction from 62.3 ° of the perimeter versus "position" i. e. the angular position of the rod (refer to the sketch, Fig. 3). The eccentricity, E, is parameter in all the graphs.

It is obvious that eccentricity has a very pronounced effect on the circumferential distribution of the rod film flow: The greater the eccentricity the more uneven the film flow rate. The maximum film flow rate occurs at the maximum gap width (position 1). For the highest eccentricity (E = 3 mm) the minimum film flow rate (occuring at the minimum gap, position 4) is very close to zero.

The total rod film flow rates, $\dot{M}_f$, have been computed by assuming film flow symmetry around the geometrical line of symmetry. The results are summarized in table 3. In Figs. 13 and 14 these results are displayed as a function of the steam quality x for G = 602 and 1200 kg /m^{2}s respectively. Also shown in these graphs are the burn-out qualities for q'' = 100.7 w/cm^2 obtained by linear interpolation in plots of measured values of x_{BO} versus q''_{BO} . Since for long heated lengths x_{BO} versus q_{BO} is almost independent of the heated length then the burn-out qualities thus obtained are realistic estimates of the actual burn-out qualities at the two relevant mass velocities and q'' = 100.1 w/cm^2. Figs. 13 and 14 may therefore be interpreted as displaying the decrease of the relative total rod film flow rate as one moves vertically upward a long heated rod. The approximate 45° slopes of the lines connecting the experimental points indicate that evaporation controls film depletion.

Examining Fig. 13 for G = 1200 kg/m^{2}s it seems clear that total film flow rate controls burn-out: burn-out occurs when the total film flow rate becomes zero. The lower burn-out qualities observed for the eccentric geometries must then be explained by the corresponding lower total film flows rather than by the uneven distribution of the film around the rod perimeter.

This conclusion is not intirely contradicted by Fig. 14 for G = 602 kg/m^{2}s although the picture here is less clear.

The experimental data for tube film flow are summarized in table 4. Figs. 15 through 18 show the angular distribution of tube film flow. The effect of eccentricity is almost as pronounced as for the rod film and the lowest film flow rate is also here found in the narrow gap (pos. 4). The total tube film flow rate is not very dependent upon eccentricity. This is in contrast to what was found for the rod film flow rate for G = 1200 kg/m^{2}s.

3.3. Frictional Pressure Drop.

In Figs. 19 to 23 is given the result of the diabatic pressure drop measurements at 70 bar for a constant heat flux q''=100.7 W/cm^2 and two values of flow, G = 600 kg/m^{2}s and 1200 kg/m^{2}s. The figures are given with the eccentricity E as parameter.

The multiplier is determined from the total pressure drop corrected for the influence of the hydrostatic head by means of the Bankoff-Jones void formula. The single phase pressure drop as determined from measurements has been expressed as

$$\left(\frac{dp}{dz}\right)_{friction} = 0.40\ Re^{-0.25}\ \frac{1}{D_H}\ \frac{G^2}{2\rho_1}$$

It can be seen from the figures that the influence of eccentricity is small. However, a slight decrease in the frictional pressure drop may be observed for increasing eccentricity.

4. Conclusions.

Experiments with a 17×27.2×3500 mm annulus geometry with heated rod have led to the following preliminary conclusions:

1. Rod eccentricity has a pronounced adverse effect on burn-out at mass velocities greater than 500 kg/m^{2}s. At smaller mass velocities eccentricity may have a small beneficial effect at small subcoolings.

2. The circumferential variation of the rod and tube film flow rate becomes increasingly pronounced for increasing eccentricity. The film flow rate is smallest in the narrow gap. The rod film flow becomes close to zero at the highest eccentricity (3 mm) even at steam qualities rather far removed from the burn-out quality.

3. The total rod film flow rate decreases with increasing eccentricity for G = 1200 kg/m^{2}s, but remains relatively unaffected at G = 602 kg/m^{2}s.

4. Burn-out performance seems primarily to be controlled by the total rod film flow rate.

5. Eccentricity has possibly a small (beneficial) effect on the pressure drop.

5. Nomenclature.

D_H	hydraulic diameter
E	eccentricity
G	mass velocity
$\dot{M}_f$	total film flow rate
$\dot{m}_f$	film flow rate ("partial suction")
$\dot{m}_s$	steam flow rate("partial suction")
$\dot{m}_w$	water flow rate ("partial suction")
p	pressure
Q	total power
q''	specific power
$Re = GD_H/\mu$	Reynolds number
x	steam quality
x_o	steam quality at outlet
z	axial coordinate
Δt_{sub}	inlet subcooling
ϱ_l	density of liquid
φ	two-phase multiplier
μ	dynamic viscosity

6. References.

1. Butterworth, D. : Air-water climbing film flow in an eccentric annulus. U. K. A. E. A., Report No. AERE-R5787 (May 1968).

2. Schraub, F. A. et al.: GEAP-5739 (1969).

3. Jensen, A., Olsen, A., Mannov, G., Seir Olsen. J., Hartig, A. Risø-M-1384.

Pressure: P = 70 BAR

q''_{rod} w/cm^2	G kg/m^{2}s	x_o %	Pos. 1	Pos. 2.5		E mm
100.7	602	23.9	(3.6) 3.6	3.6	[2.9]	0
100.7	602	19.0	(5.2)		[3.6]	0
100.8	1200	23.2	(5.6) 5.8	5.0		0
100.7	1201	20.2	(7.4)		[5.2]	0

q''_{rod} w/cm^2	G kg/m^{2}s	x_o %	Pos. 1		Pos. 2		Pos. 3		Pos.4		E mm
100.7	602	23.9	(5.6)	5.7	(3.7)	4.8	(2.6)	3.7	(2.1)	3.0	1.5
				6.3		4.5		2.5		1.8	2.5
			(6.5)		(5.0)		(1.5)		(0.4)		3.0
100.7	602	19.0	(7.7)		(4.7)		(2.0)		(2.0)		1.5
			(9.2)		(5.3)		(1.0)		(1.0)		3.0
100.8	1200	23.2		6.6		5.2		4.3		3.5	1.5
				4.5		3.8		3.2		2.5	2.5
							(3.0)				3.0
100.7	1201	20.2	(5.8)		(6.5)		(4.3)		(3.6)		1.5
			(9.2)		(7.9)		(2.4)		(-)		3.0

Numbers in [] brackets: Exp. period No. 3.

Numbers in () brackets: Exp. period No. 4.

Numbers without brackets: Exp. period No. 5.

(Exp. period No. 3 corresponds to suction from the total perimeter. For fin configurations corresponding to Exp. periods No. 4 and 5 see fig. 1).

Table 2 : Rod film flow rates on 62.3° in g/s.

G [kg/m^{2}s]	E [mm]	x [%]	$\dot{M}_f$ [g/s]	$\dot{M}_f/\dot{M}_{TOT}$ [%]
602	o ¤)	24.4	16.8	7.9
	o	23.7	20.8	9.8
	1.5	23.8	22.2	10.4
	2.5	24.0	21.3	10.0
	3	23.8	19.2	9.0
	o ¤)	19.5	20.8	9.8
	o	19.0	30.0	14.1
	1.5	18.7	22.2	10.4
	3.0	18.9	22.0	10.3
1200	o	22.9	33.5	7.9
	1.5	22.9	28.0	6.6
	2.5	23.6	20.2	4.8
	3.0	23.2	17.3	4.1
	o ¤)	20.2	30.0	7.1
	o	20.1	42.8	10.1
	1.5	20.1	29.9	7.0
	3.0	20.2	28.7	6.8

Table 3. Total rod film flow rates. ¤) Suction from 360°.

Pressure: P = 70 BAR

q''_{rod} w/cm^2	G kg/m^{2}s	x_o %	Pos. 1		Pos. 2.5		E mm
100.7	602	23.7	(20.5)	21.4	19.0	[20.0]	0
100.7	603	18.9	(20.6)			[20.6]	0
100.9	1201	23.1		31.0	31.0		0
100.6	1201	20.1	(27.8)			[28.5]	0

q''_{rod} w/cm^2	G kg/m^{2}s	x_o %	Pos. 1		Pos. 2		Pos. 3		Pos. 4		E mm
100.7	602	23.7	(24.0)	33.0	(24.0)	24.3	(16.4)	21.5	(13.5)	18.3	1.5
				31.2		26.0		16.1		9.6	2.5
			(29.0)		(26.4)		(15.5)		(9.0)		3.0
100.7	603	18.9	(23.5)		(22.1)		(16.1)		(13.0)		1.5
			(31.0)		(25.0)		(16.5)		(7.0)		3.0
100.9	1201	23.1		35.0		36.5		33.0		27.0	1.5
				35.4		36.4		24.8		17.3	2.5
							(25.2)				3.0
100.6	1201	20.1	(39.4)		(35.0)		(29.0)		(24.3)		1.5
			(35.5)		(35.5)		(23.5)		(8.0)		3.0

Numbers in [ ] brackets: Exp. period No. 3.

Numbers in ( ) brackets: Exp. Period No. 4.

Numbers without brackets: Exp. period No. 5.

(Exp. period No. 3 corresponds to suction from the total perimeter. For fin configurations corresponding to Exp. periods No. 4 and 5 see fig. 2).

Table 4: Tube film flow rates on 62.9° in g/s.

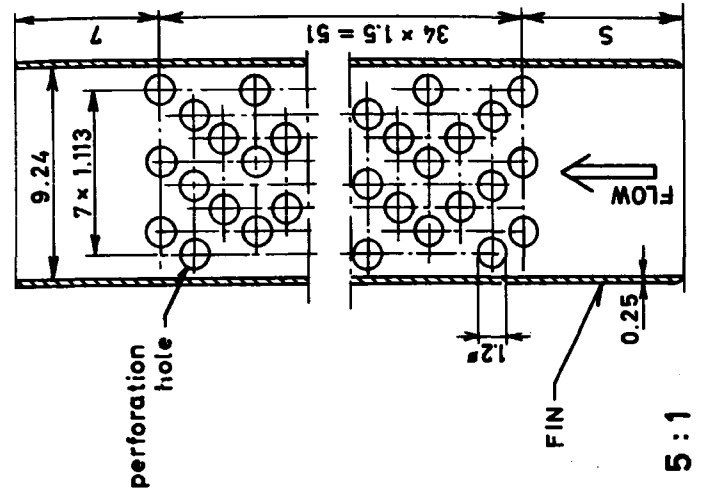

FOLD-OUT OF EXTERNAL SURFACE

5 : 1

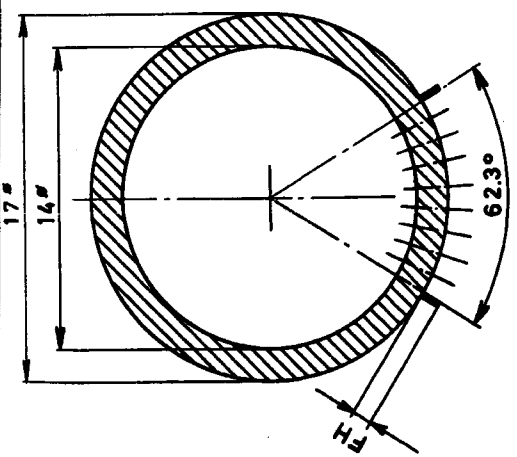

EXP. PERIOD	FH	S
4	0.5	5.0
5	1.0	8.0

ROD SUCTION PERFORATION

Fig.1

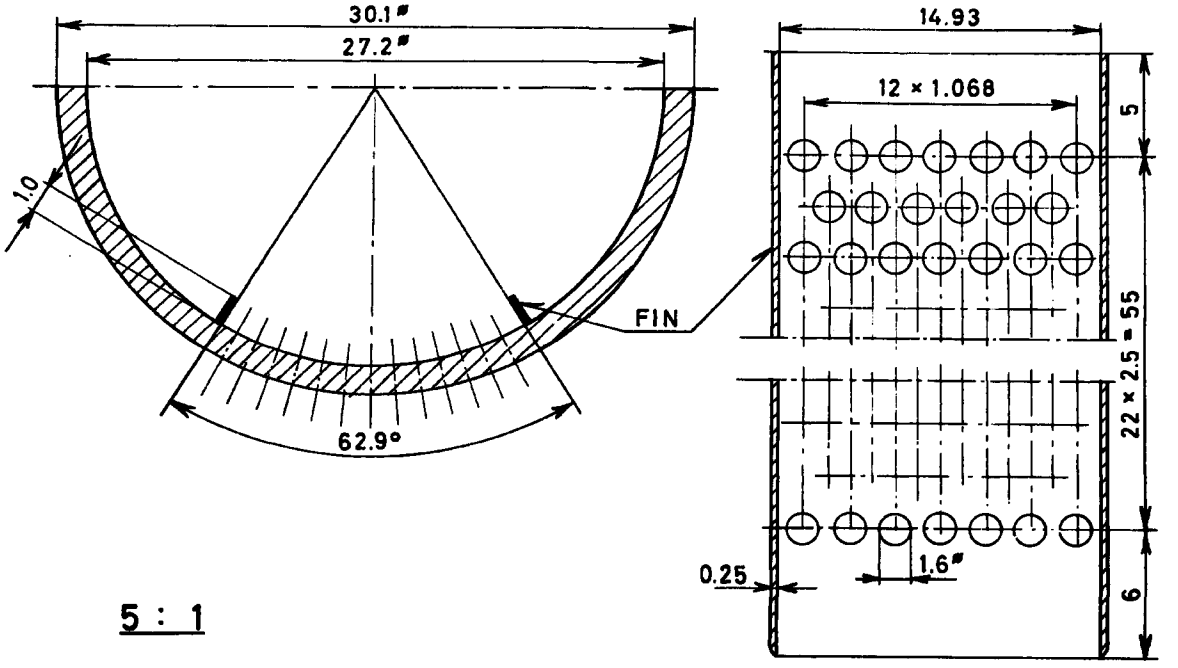

TUBE SUCTION PERFORATION

Fig. 2

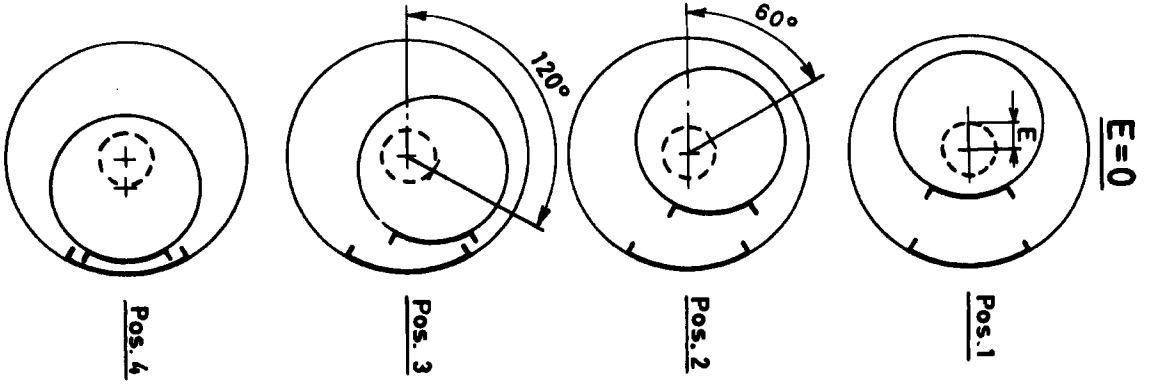

SKETCH OF EXPERIMENTAL ROD POSITIONS

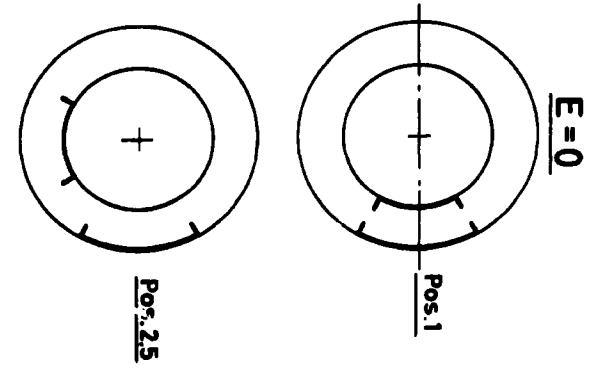

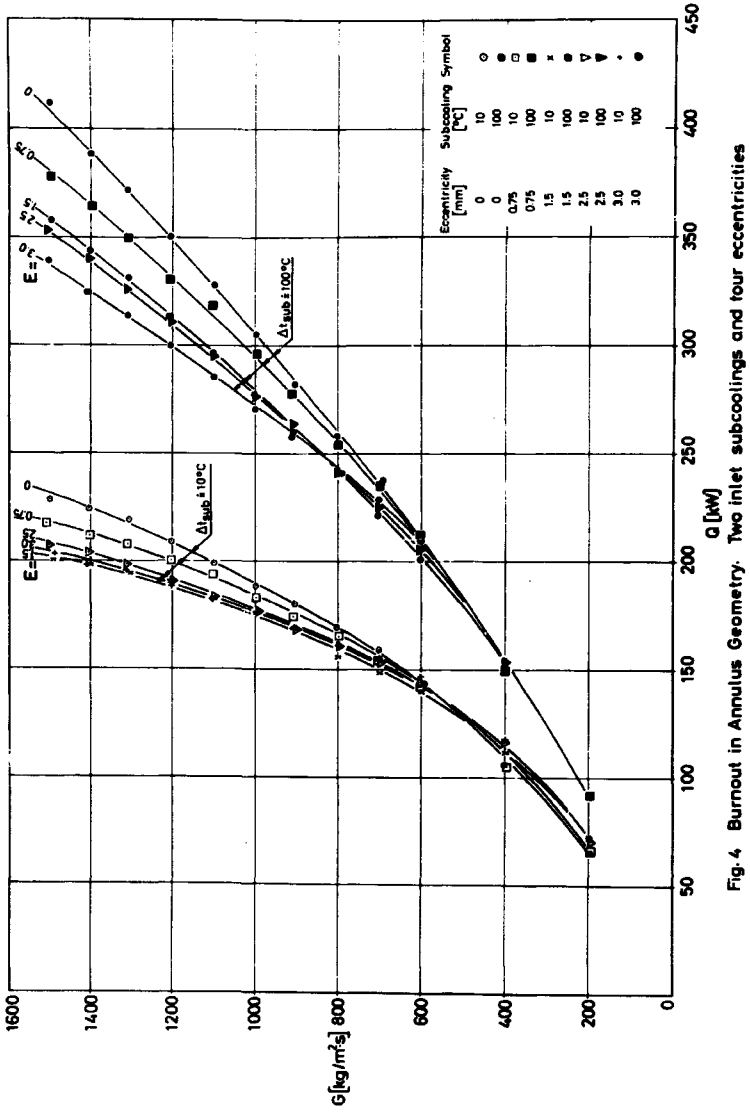

Fig. 4 Burnout in Annulus Geometry. Two inlet subcoolings and four eccentricities

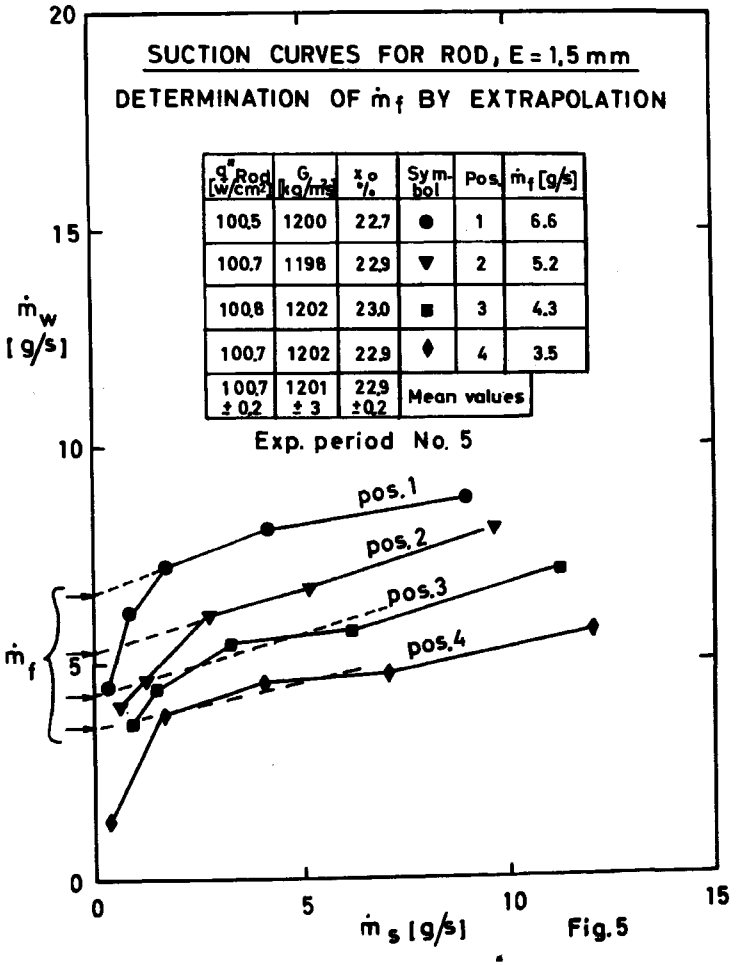

Fig. 5

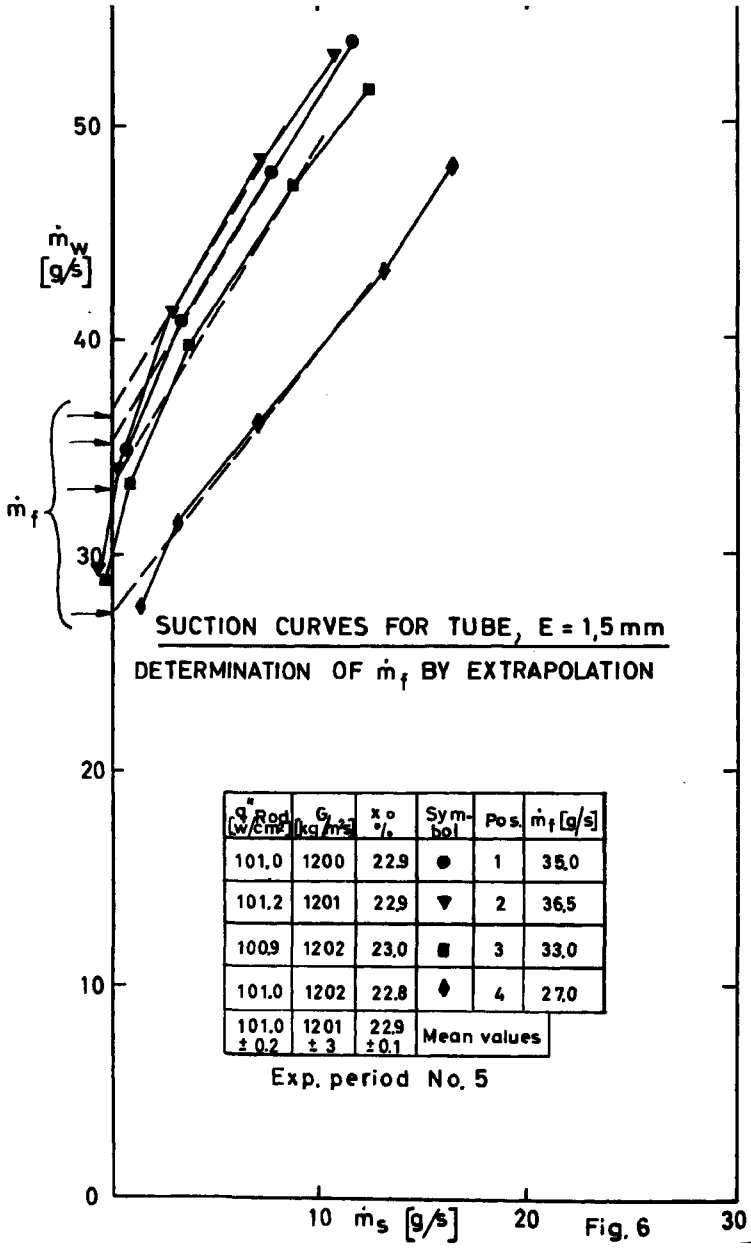

SUCTION CURVES FOR TUBE, E = 1,5 mm

DETERMINATION OF $\dot{m}_f$ BY EXTRAPOLATION

q''_{Rod} [w/cm²]	G [kg/m²s]	x_o %	Symbol	Pos.	$\dot{m}_f$ [g/s]
101,0	1200	22,9	●	1	35,0
101,2	1201	22,9	▼	2	36,5
100,9	1202	23,0	■	3	33,0
101,0	1202	22,8	♦	4	27,0
101,0 ± 0,2	1201 ± 3	22,9 ± 0,1	Mean values		

Exp. period No. 5

Fig. 6

SUCTION CURVES FOR ROD, E = 0

COMPARISON BETWEEN DIFFERENT SUCTION PROCEDURES

Exp. period	q''_{rod} w/cm²	G kg/m²s	x_o %	Suction from	Symbol
4	100,4	601	23,7	pos.1	⊙
5	100,9	602	23,7	pos.1	●
5	101,3	603	23,6	pos.2-5	▲
3	101,0	600	24,4	total perimeter	x

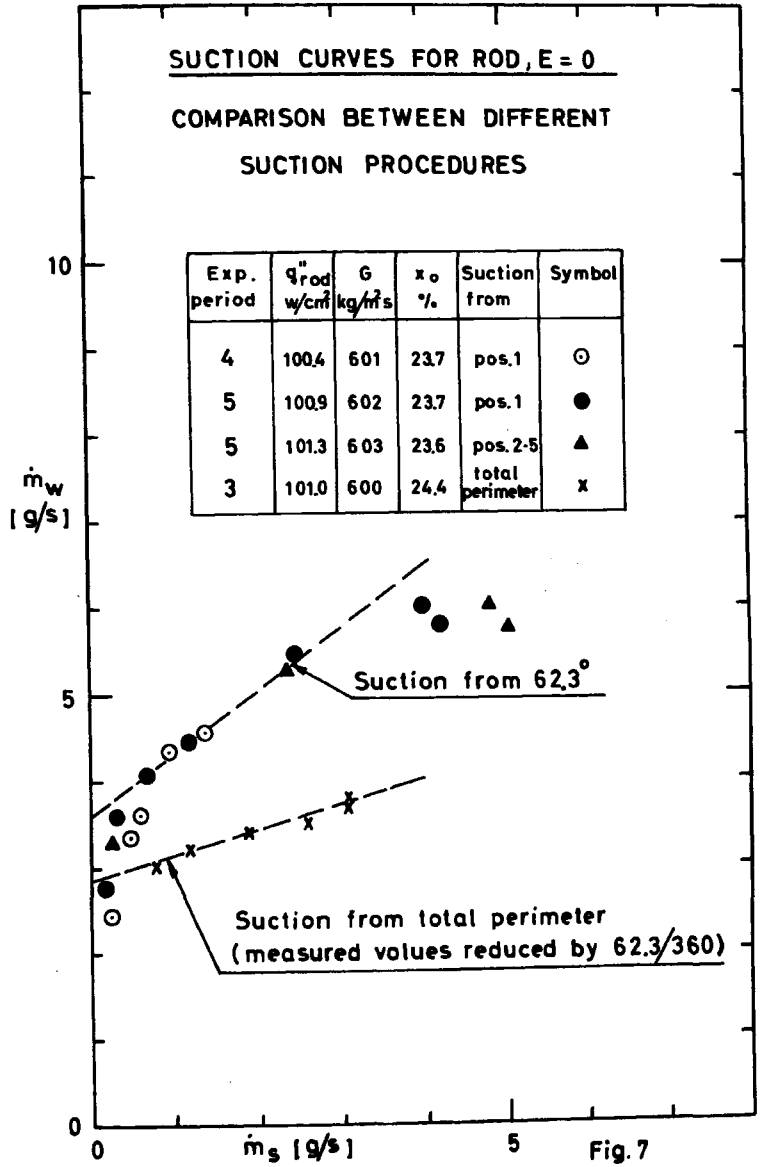

Fig. 7

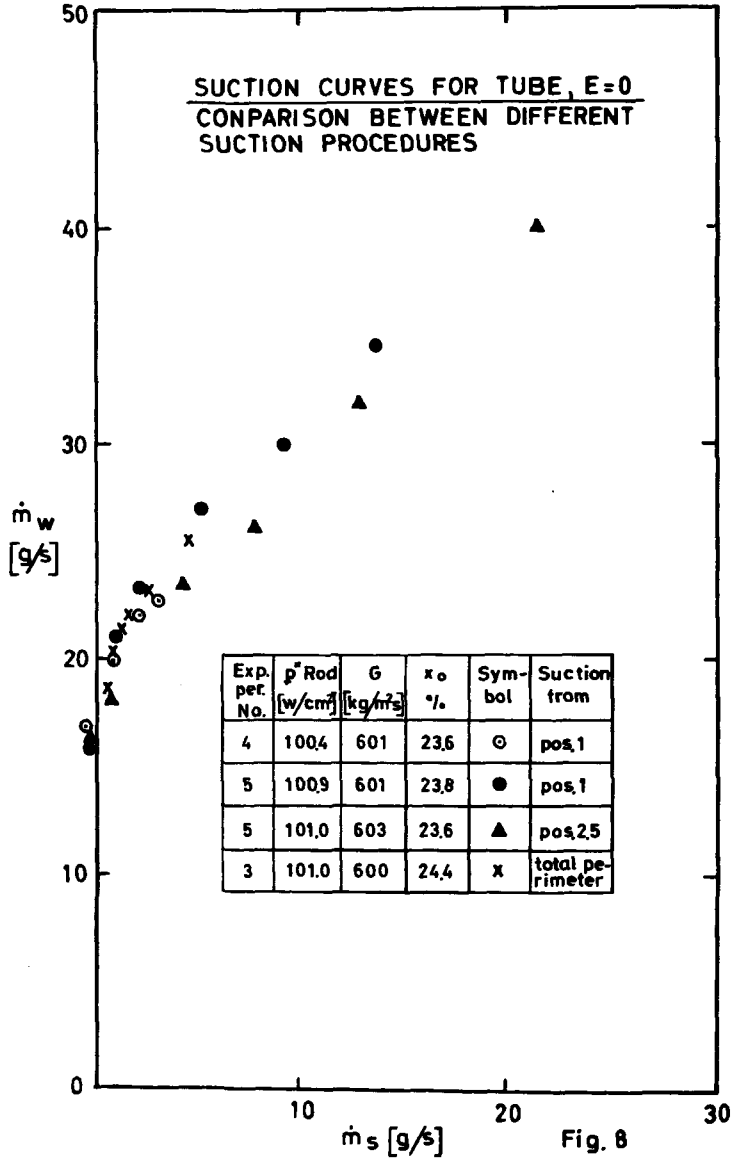

Exp. per. No.	p" Rod [w/cm²]	G [kg/m²s]	x_o %	Sym-bol	Suction from
4	100,4	601	23,6	⊙	pos,1
5	100,9	601	23,8	●	pos,1
5	101,0	603	23,6	▲	pos,2,5
3	101,0	600	24,4	x	total perimeter

Fig. 8

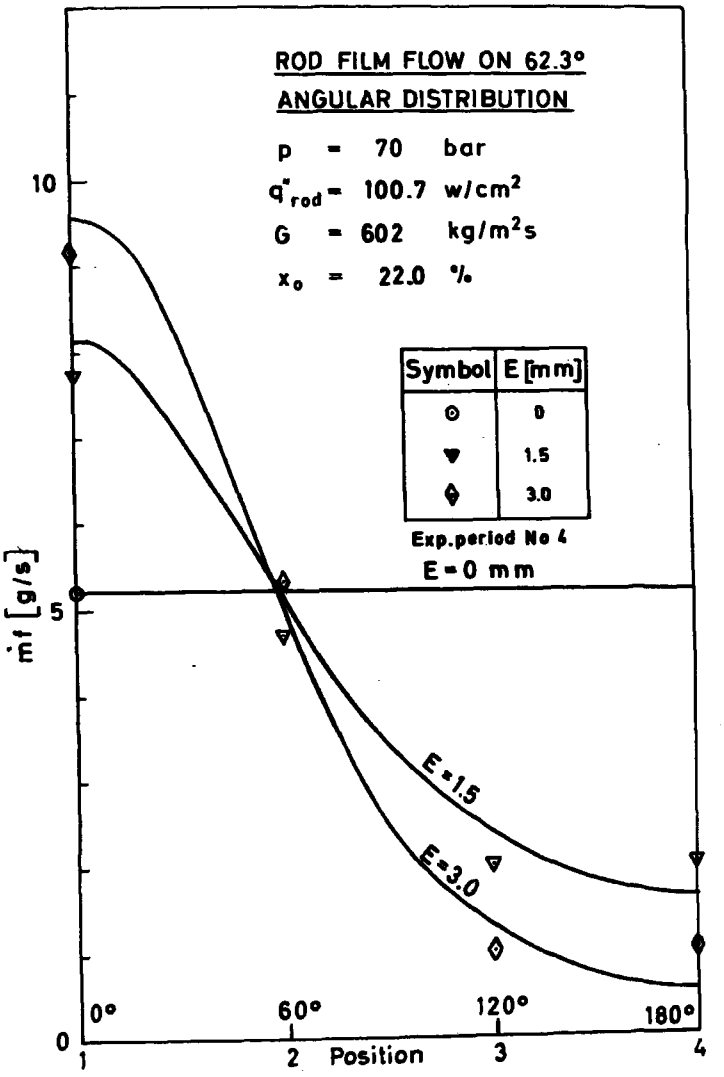

Fig.9

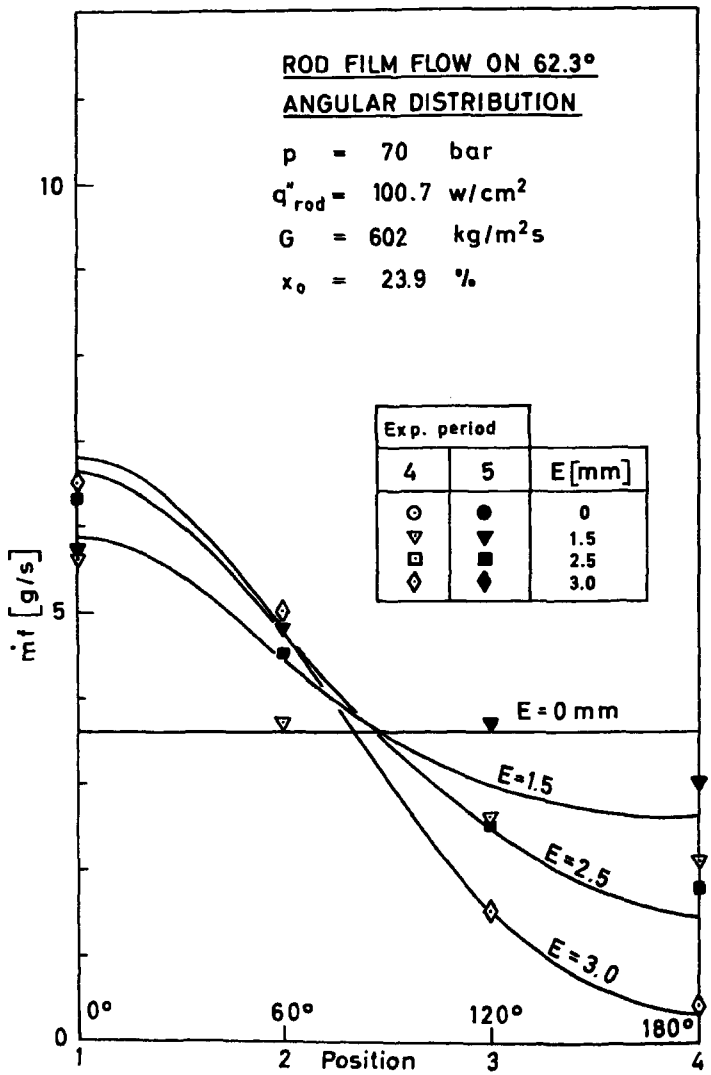
ROD FILM FLOW ON 62.3°
ANGULAR DISTRIBUTION
p = 70 bar
q"rod = 100.7 w/cm²
G = 602 kg/m²s
xo = 23.9 %
Exp. period
4
5
E[mm]
0
1.5
2.5
3.0
E = 0 mm
E=1.5
E=2.5
E=3.0
ṁf [g/s]
10
5
0
0°
60°
120°
180°
1
2
Position
3
4

Fig.10

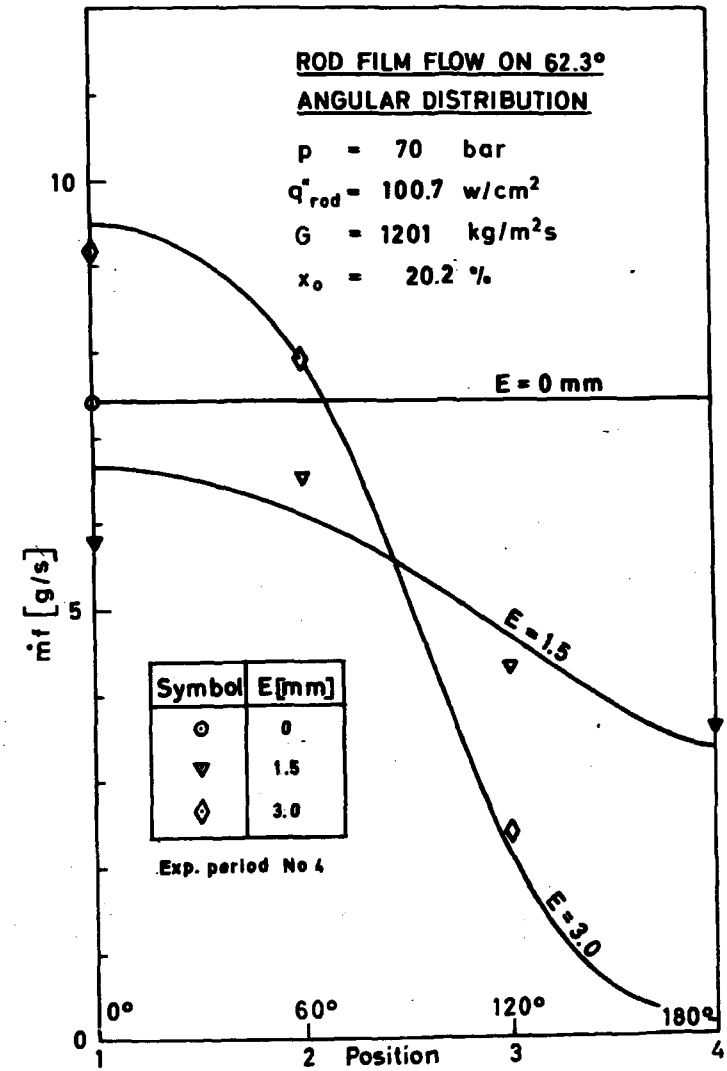
ROD FILM FLOW ON 62.3°
ANGULAR DISTRIBUTION
p = 70 bar
q"rod = 100.7 w/cm²
G = 1201 kg/m²s
xo = 20.2 %
E = 0 mm
E=1.5
E=3.0
Symbol
E[mm]
0
1.5
3.0
Exp. period No 4
ṁf [g/s]
10
5
0
0°
60°
120°
180°
1
2
Position
3
4

Fig.11

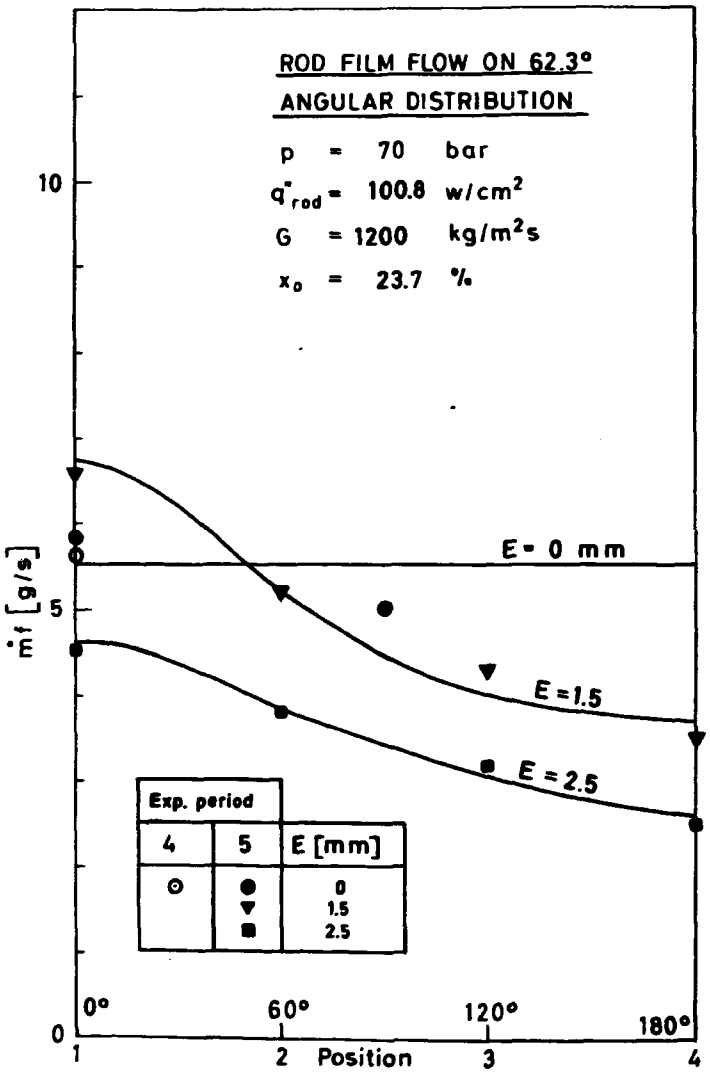
ROD FILM FLOW ON 62.3°
ANGULAR DISTRIBUTION
p = 70 bar
q"rod = 100.8 w/cm²
G = 1200 kg/m²s
x₀ = 23.7 %
ṁf [g/s]
E = 0 mm
E = 1.5
E = 2.5
Exp. period
4
5
E [mm]
0
1.5
2.5
0°
60°
120°
180°
Position

Fig. 12

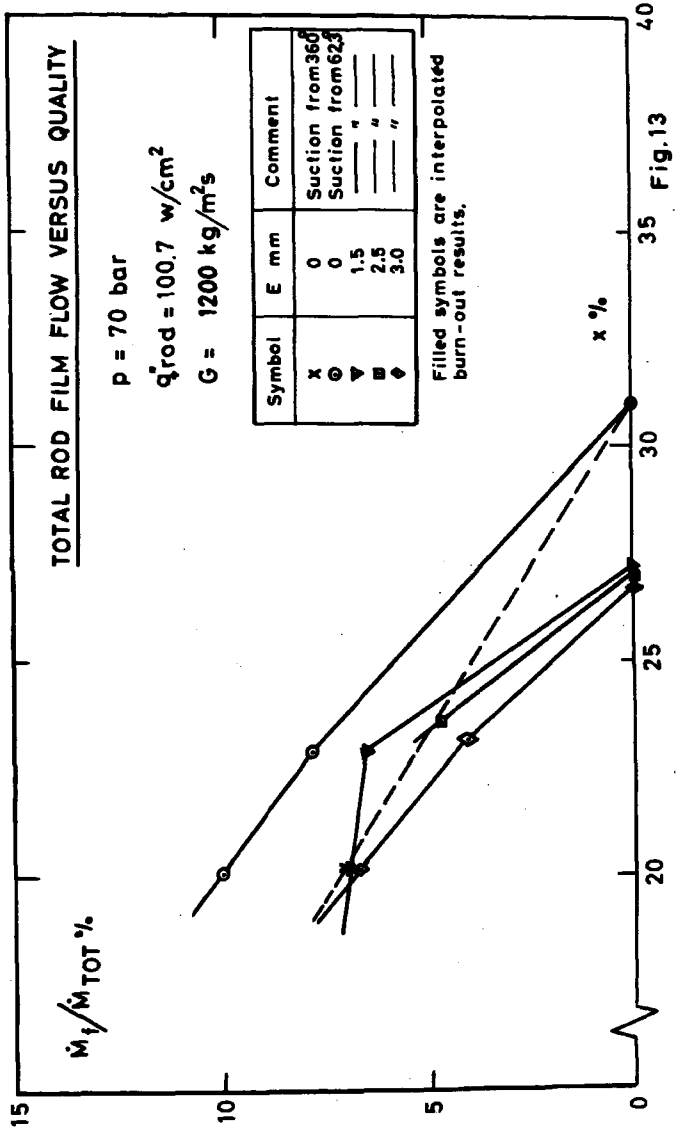
TOTAL ROD FILM FLOW VERSUS QUALITY
p = 70 bar
q"rod = 100.7 w/cm²
G = 1200 kg/m²s
Symbol
E mm
Comment
Suction from360
Suction from623
Filled symbols are interpolated burn-out results.
x %
Ṁf/ṀTOT %

Fig. 13

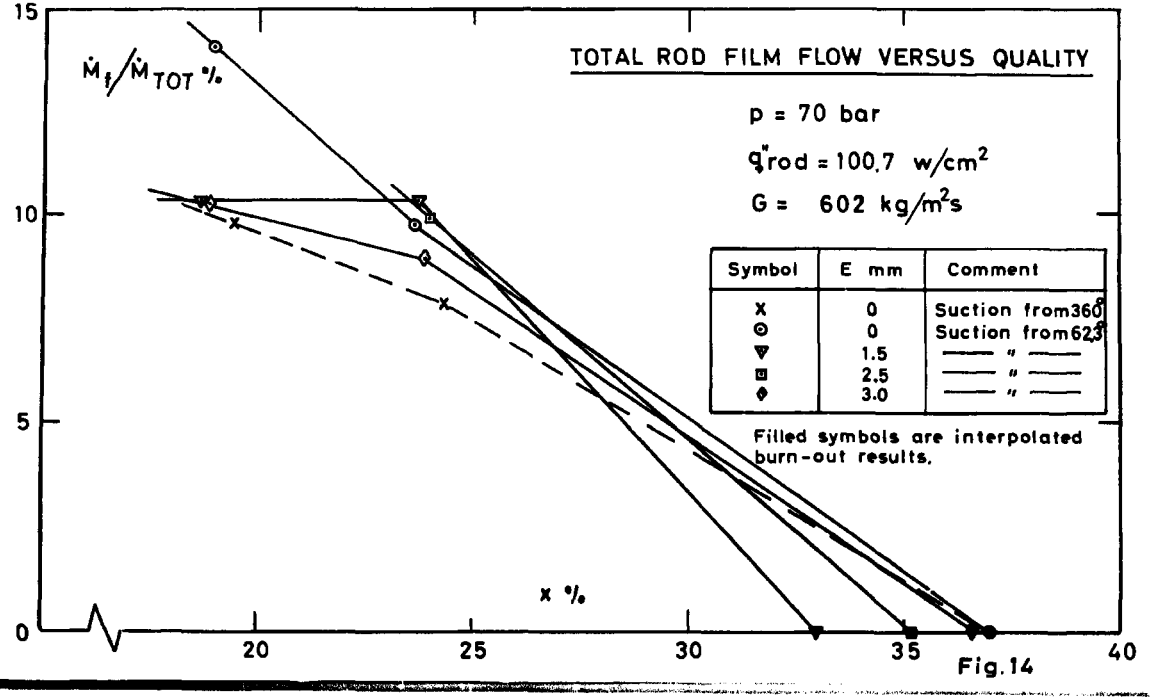
TOTAL ROD FILM FLOW VERSUS QUALITY
p = 70 bar
q"rod = 100.7 w/cm²
G = 602 kg/m²s
Symbol | E mm | Comment
0 | Suction from360°
0 | Suction from623°
1.5 | " "
2.5 | " "
3.0 | " "
Filled symbols are interpolated burn-out results.
Ṁf/ṀTOT %
x %
0
5
10
15
20
25
30
35
40

Fig. 14

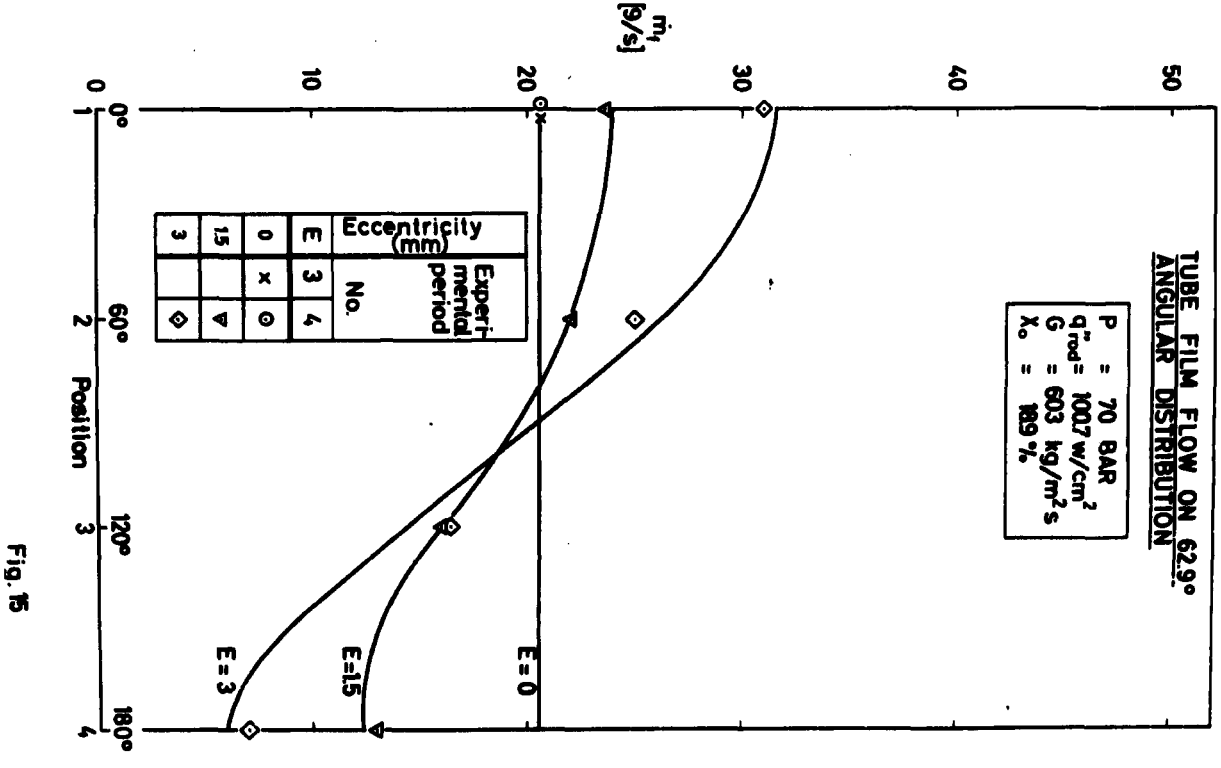
TUBE FILM FLOW ON 62.9° ANGULAR DISTRIBUTION
P = 70 BAR
q"rod = 100.7 w/cm²
G = 603 kg/m²s
Xo = 18.9 %
Eccentricity (mm)
E | 3 | 1.5 | 0
Experimental period No. 3 | x | x | x
Experimental period No. 4 | ◇ | ▽ | ○
E=3
E=1.5
E=0
Position
0°
60°
120°
180°
1
2
3
4
0
10
20
30
40
50
ṁf [g/s]

Fig. 15

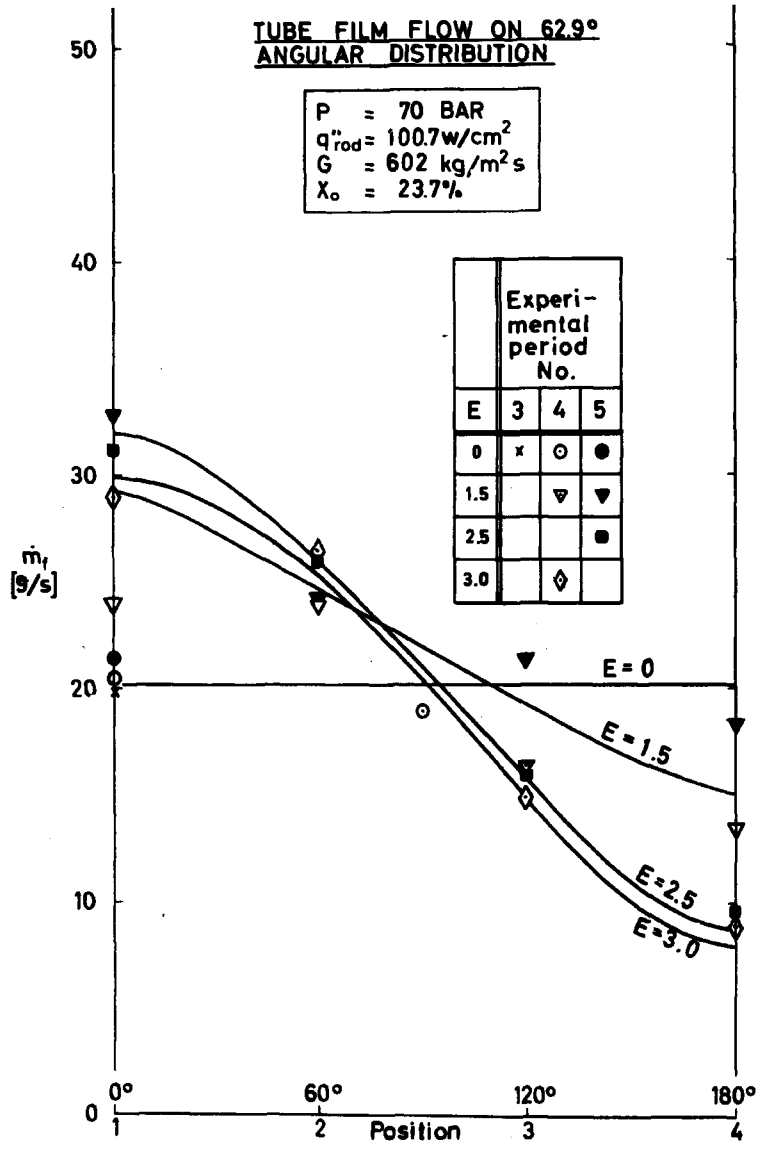
TUBE FILM FLOW ON 62.9°
ANGULAR DISTRIBUTION
P = 70 BAR
q"rod = 100.7 w/cm²
G = 602 kg/m²s
Xo = 23.7%
Experimental period No.
E
3
4
5
0
1.5
2.5
3.0
ṁf [g/s]
E = 0
E = 1.5
E = 2.5
E = 3.0
0°
60°
120°
180°
Position
1
2
3
4
0
10
20
30
40
50

Fig. 16

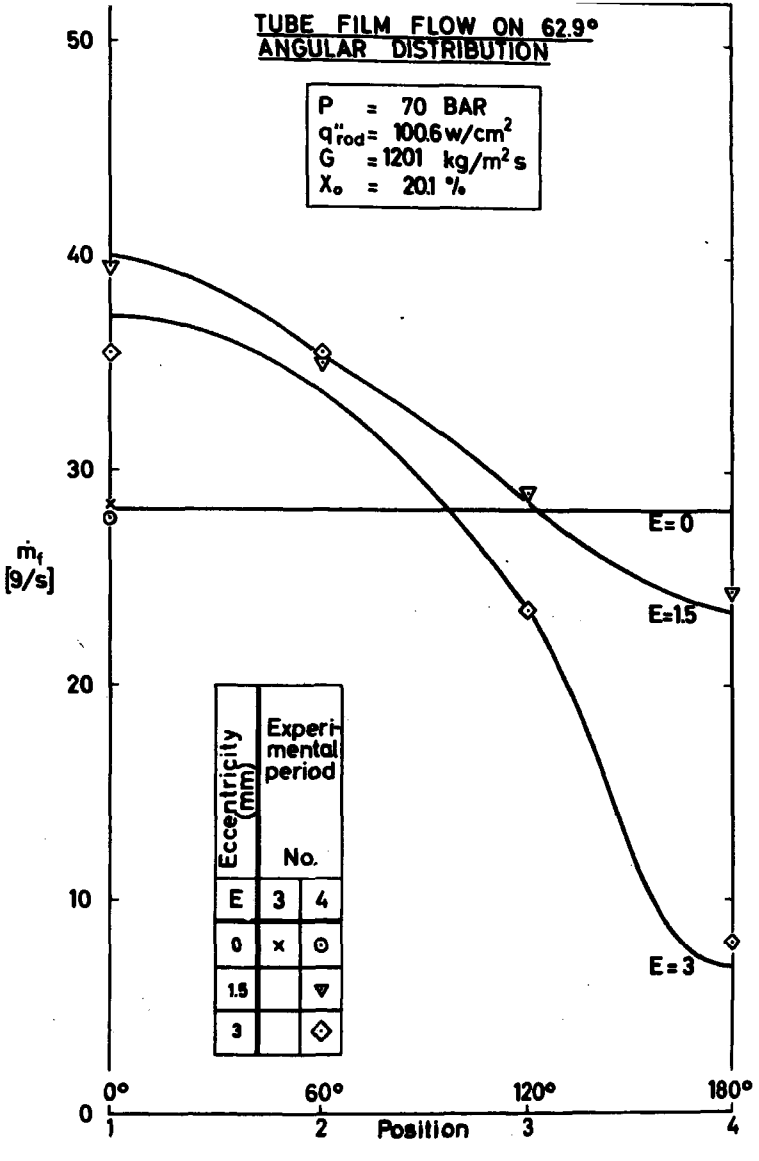
TUBE FILM FLOW ON 62.9°
ANGULAR DISTRIBUTION
P = 70 BAR
q"rod = 100.6 w/cm²
G = 1201 kg/m²s
Xo = 20.1 %
Eccentricity (mm)
Experimental period No.
E
3
4
0
1.5
3
ṁf [g/s]
E = 0
E = 1.5
E = 3
0°
60°
120°
180°
Position
1
2
3
4
0
10
20
30
40
50

Fig. 17

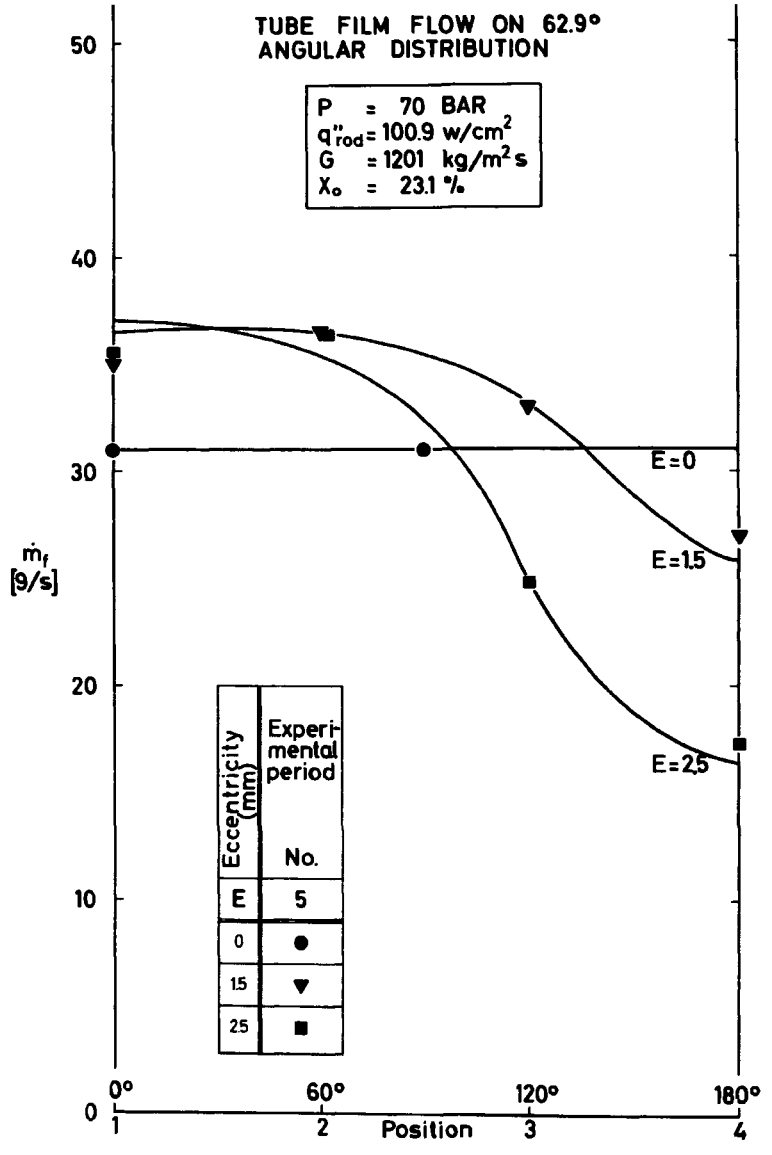
TUBE FILM FLOW ON 62.9°
ANGULAR DISTRIBUTION
P = 70 BAR
q"rod = 100.9 w/cm²
G = 1201 kg/m²s
Xo = 23.1 %
ṁf [g/s]
E=0
E=1.5
E=2.5
Eccentricity (mm)
Experimental period No.
E 5
0 ●
1.5 ▼
2.5 ■
0° 60° 120° 180°
1 2 3 4
Position

Fig. 18

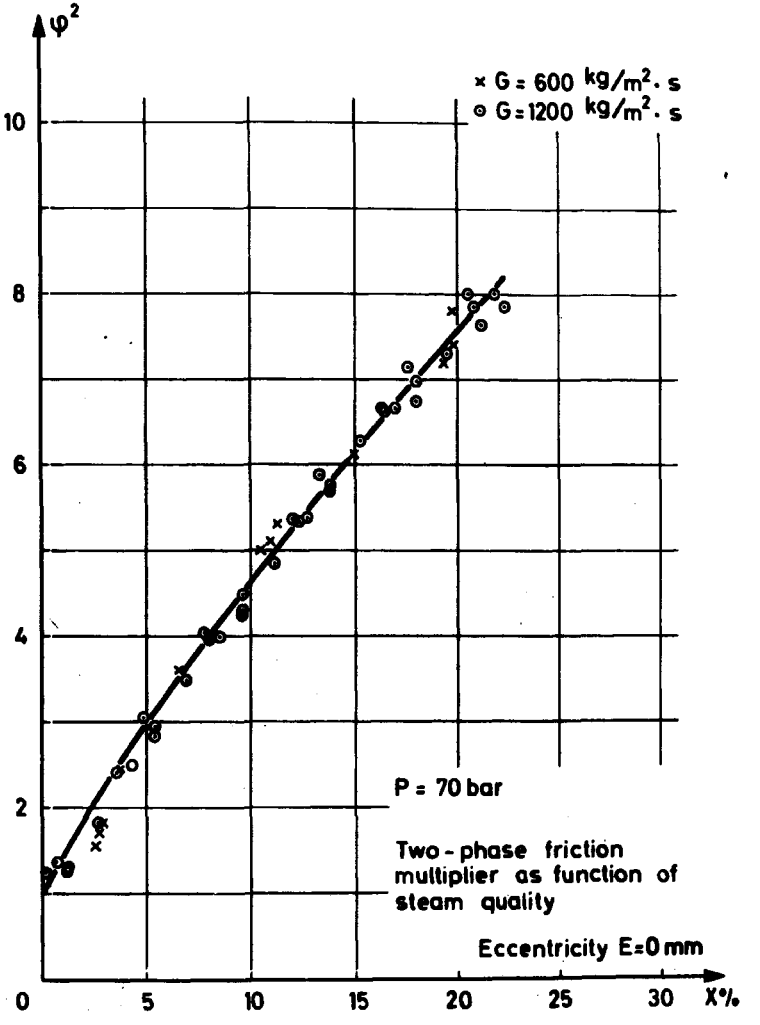
φ²
× G = 600 kg/m². s
⊙ G = 1200 kg/m². s
P = 70 bar
Two-phase friction multiplier as function of steam quality
Eccentricity E=0 mm
X%

Fig. 19

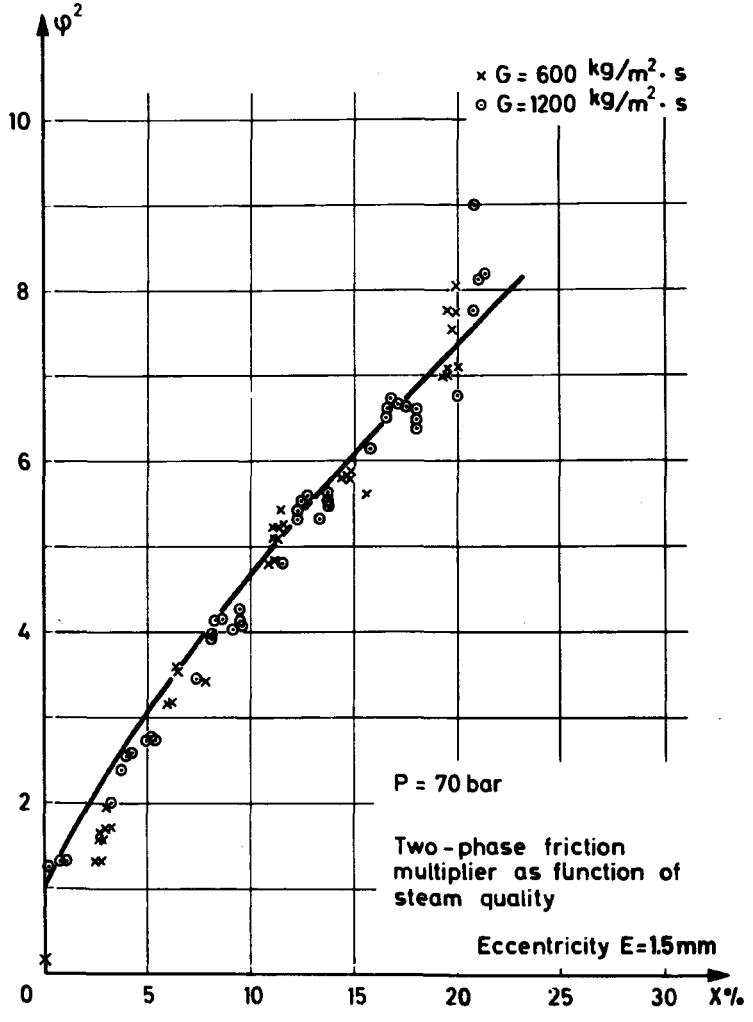
φ²
× G = 600 kg/m². s
⊙ G = 1200 kg/m². s
10
8
6
4
2
0
5
10
15
20
25
30
X%
P = 70 bar
Two-phase friction multiplier as function of steam quality
Eccentricity E=1.5mm

Fig. 20

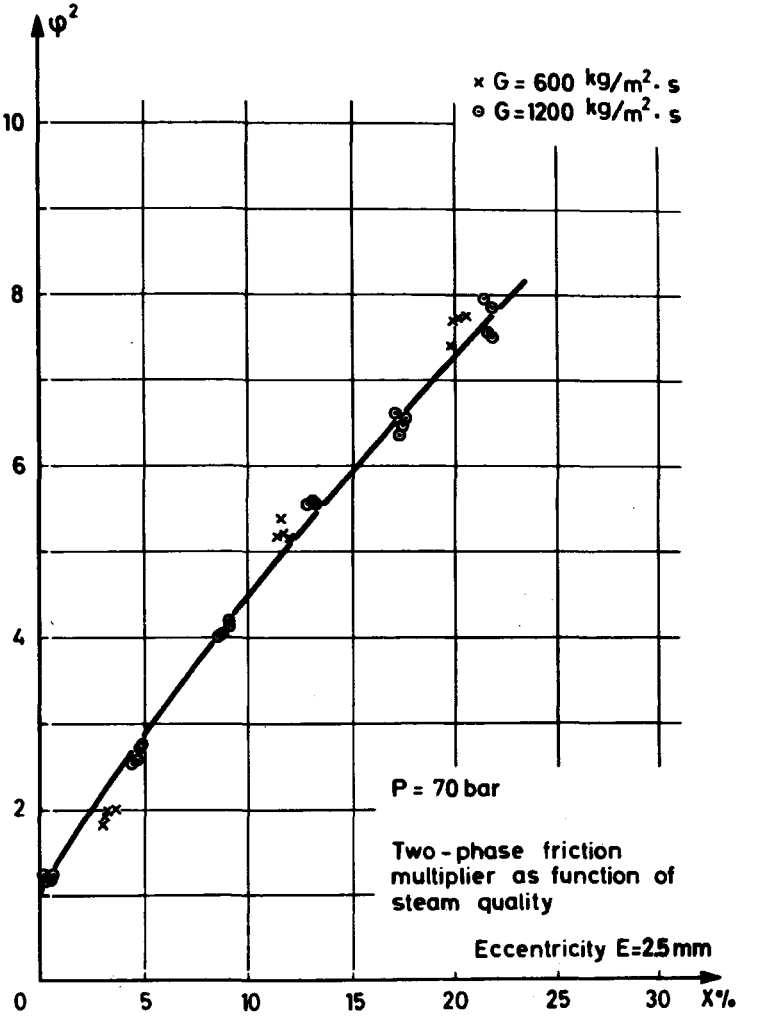
φ²
× G = 600 kg/m². s
⊙ G = 1200 kg/m². s
10
8
6
4
2
0
5
10
15
20
25
30
X%
P = 70 bar
Two-phase friction multiplier as function of steam quality
Eccentricity E=2.5mm

Fig. 21

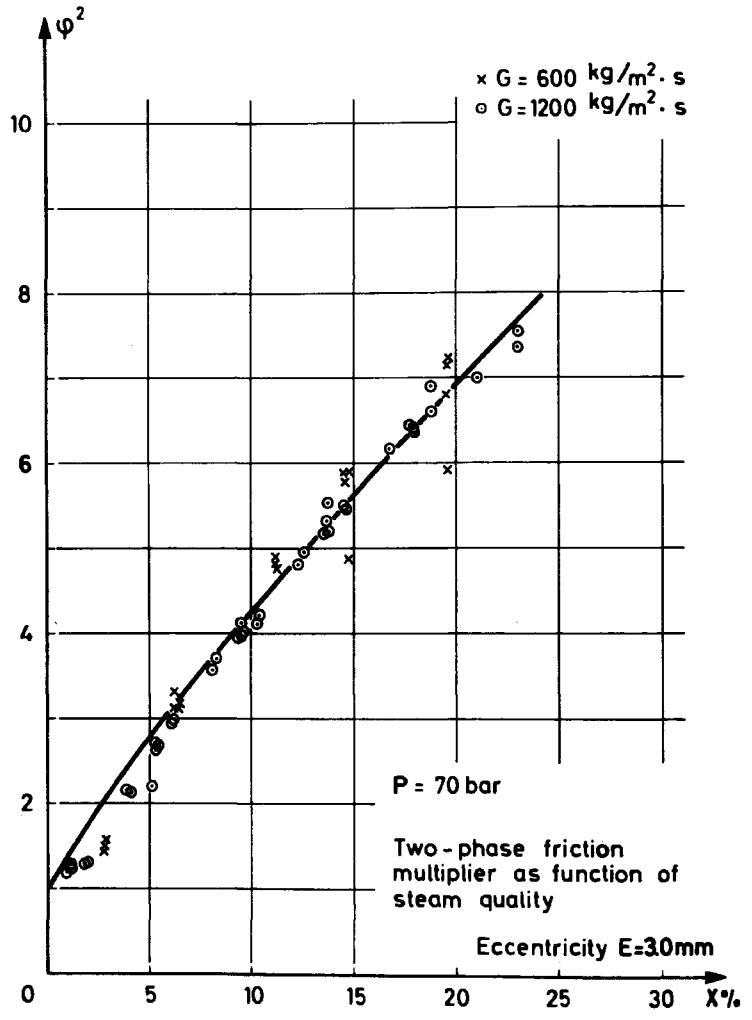
φ²
× G = 600 kg/m². s
⊙ G = 1200 kg/m². s
P = 70 bar
Two-phase friction multiplier as function of steam quality
Eccentricity E=3.0mm
X%

Fig. 22

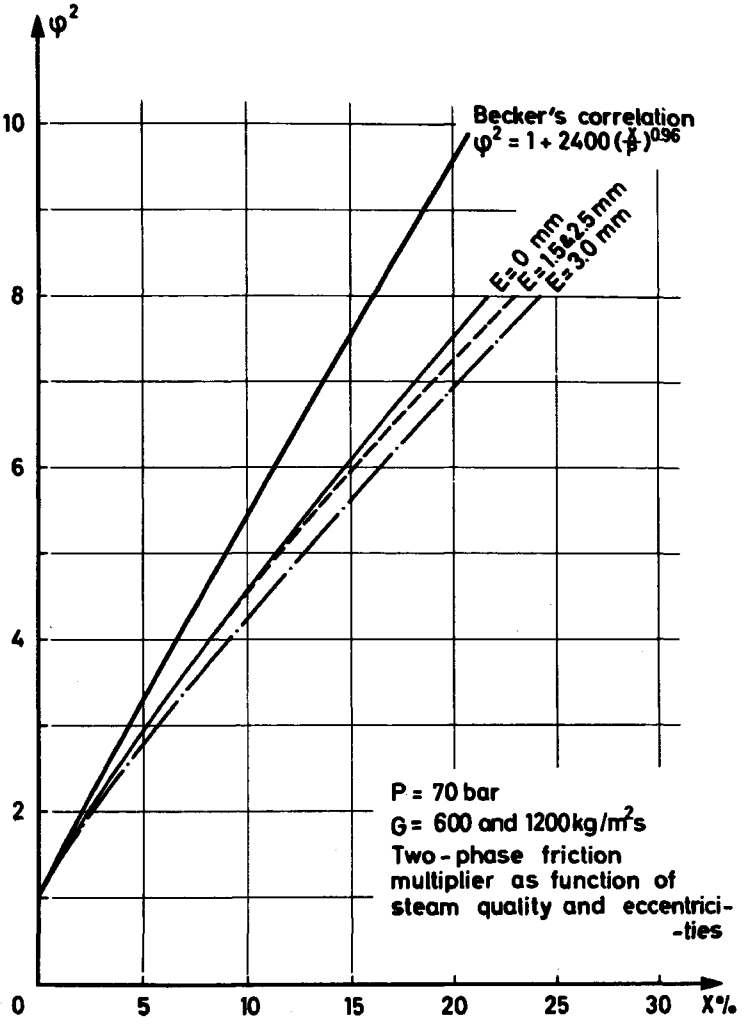
φ²
Becker's correlation
φ² = 1 + 2400 (X/β)^0.96
E = 0 mm
E = 1.5 & 2.5 mm
E = 3.0 mm
P = 70 bar
G = 600 and 1200 kg/m²s
Two-phase friction multiplier as function of steam quality and eccentricities
X%

Fig. 23